

Ezetimibe suppresses development of liver tumors by inhibiting angiogenesis in mice fed a high-fat diet

Kouichi Miura¹  | Hirohide Ohnishi^{2,3} | Naoki Morimoto¹ | Shinichiro Minami⁴ | Mitsuaki Ishioka⁴ | Shunji Watanabe¹ | Mamiko Tsukui¹ | Yoshinari Takaoka¹ | Hiroaki Nomoto¹ | Norio Isoda¹ | Hironori Yamamoto¹

¹Division of Gastroenterology, Department of Medicine, School of Medicine, Jichi Medical University, Shimotsuke, Tochigi, Japan

²Department of Gastroenterology, Saitama Medical Center, Jichi Medical University, Saitama, Japan

³Japan Organization of Occupational Health and Safety, Kanagawa, Japan

⁴Department of Gastroenterology, Akita University Graduate School of Medicine, Akita, Japan

Correspondence

Kouichi Miura, Division of Gastroenterology, Department of Medicine, School of Medicine, Jichi Medical University, Shimotsuke, Tochigi, Japan.
Email: miura385@jichi.ac.jp

Funding information

Bayer

Nonalcoholic steatohepatitis (NASH) is a common cause of liver cirrhosis and hepatocellular carcinoma (HCC). However, effective therapeutic strategies for preventing and treating NASH-mediated liver cirrhosis and HCC are lacking. Cholesterol is closely associated with vascular endothelial growth factor (VEGF), a key factor that promotes HCC. Recent reports have demonstrated that statins could prevent HCC development. In contrast, we have little information on ezetimibe, an inhibitor of cholesterol absorption, in regards to the prevention of NASH-related liver cirrhosis and HCC. In the present study, a steatohepatitis-related HCC model, hepatocyte-specific phosphatase and tensin homolog (*Pten*)-deficient (*Pten*^{Δ_{hep}) mice were fed a high-fat (HF) diet with/without ezetimibe. In the standard-diet group, ezetimibe did not reduce the development of liver tumors in *Pten*^{Δ_{hep} mice, in which the increase of serum cholesterol levels was mild. Feeding of a HF diet increased serum cholesterol levels markedly and subsequently increased serum levels of VEGF, a crucial component of angiogenesis. The HF diet increased the number of VEGF-positive cells and vascular endothelial cells in the tumors of *Pten*^{Δ_{hep} mice. Kupffer cells, macrophages in the liver, increased VEGF expression in response to fat overload. Ezetimibe treatment lowered cholesterol levels and these angiogenic processes. As a result, ezetimibe also suppressed inflammation, liver fibrosis and tumor growth in *Pten*^{Δ_{hep} mice on the HF diet. Tumor cells were highly proliferative with HF-diet feeding, which was inhibited by ezetimibe. In conclusion, ezetimibe suppressed development of liver tumors by inhibiting angiogenesis in *Pten*^{Δ_{hep} mice with hypercholesterolemia.}}}}}

KEYWORDS

angiogenesis, hepatocellular carcinoma, hypercholesterolemia, nonalcoholic steatohepatitis, vascular endothelial growth factor

1 | INTRODUCTION

Nonalcoholic steatohepatitis (NASH) is an advanced manifestation of the liver in the metabolic syndrome. NASH is one of the most common causes of liver cirrhosis and hepatocellular carcinoma (HCC). As a result,

NASH is one of the leading causes of liver transplantation for advanced liver diseases in the developed countries, including the United States.¹ However, effective therapeutic strategies for preventing and treating NASH have not been developed. Thus, urgent action is required to reduce the prevalence of NASH and its associated comorbidities.

This is an open access article under the terms of the Creative Commons Attribution-NonCommercial License, which permits use, distribution and reproduction in any medium, provided the original work is properly cited and is not used for commercial purposes.

© 2018 The Authors. *Cancer Science* published by John Wiley & Sons Australia, Ltd on behalf of Japanese Cancer Association.

Excess intake of fat from the diet has been shown in clinical studies to be closely associated with NASH development.² “Fat overload” has been shown to promote NASH in experimental animal models.³ Of the different types of lipids, cholesterol overload promotes NASH progression in humans,^{4,5} even though cholesterol is an essential component of cell membranes and steroid hormones. Indeed, greater deposition of cholesterol has been noted in NASH livers than in simple steatosis.⁴ In addition, hypercholesterolemia has been shown to be associated with HCC development in patients with type-2 diabetes mellitus.⁶ Furthermore, cholesterol consumption can increase the risk of liver cancer.⁷ Thus, hypercholesterolemia caused by excess fat intake is a risk factor that exacerbates NASH and NASH-related HCC.

Several mechanisms by which cholesterol promotes NASH have been shown in experimental models. For instance, cholesterol accumulation in hepatocytes depletes glutathione levels in mitochondria, resulting in sensitization to tumor necrosis factor- α -induced cell death.⁸ Cholesterol accumulation in hepatic stellate cells promotes liver fibrosis by enhancing susceptibility to Toll-like receptor-4 ligands.⁹ Macrophages laden with cholesterol show an inflammatory phenotype and produce a large amount of pro-inflammatory cytokines.¹⁰ In addition, hypercholesterolemia is associated with high levels of vascular endothelial growth factor (VEGF),¹¹ which can promote inflammation in experimental NASH models.¹² These data suggest that normalization of cholesterol levels may reduce the development of NASH and NASH-related HCC.

Statins and ezetimibe are cholesterol-lowering agents that inhibit the synthesis and absorption of cholesterol, respectively. Several studies have shown that statins ameliorate NASH and its associated comorbidities. For instance, statins attenuate hepatic inflammation/fibrosis in human NASH.¹³ In addition, an epidemiologic study demonstrated that use of statins reduced the prevalence of HCC in patients with diabetes mellitus.¹⁴ Furthermore, the use of statins improved recurrence-free survival after curative liver resection for HCC.¹⁵ In contrast, there are conflicting data on the effects of ezetimibe, an inhibitor of cholesterol transporter Niemann-Pick C1 like protein (NPC1L1), on human NASH.^{16,17} Unfortunately, little information is available on how ezetimibe prevents NASH and its associated comorbidities.

In the present study, we examined the effects of ezetimibe on the progression of steatohepatitis and liver tumors using hepatocyte-specific phosphatase and tensin homolog (*Pten*)-deficient (*Pten* ^{Δ hep}) mice, which exhibit steatohepatitis and subsequent development of HCC.¹⁸ Phosphatase and tensin homolog is a lipid and protein phosphatase which can regulate cholesterol metabolism.¹⁸ Indeed, *Pten* ^{Δ hep} mice exhibit higher levels of serum cholesterol compared with those in control mice. In addition, *Pten* ^{Δ hep} mice do not suffer from obesity or insulin resistance, which also contribute to NASH development. Thus, *Pten* ^{Δ hep} mice are suitable for the investigation of cholesterol without the complicating effects of obesity and insulin resistance. Furthermore, *Pten* deficiency promotes tumorigenicity, and approximately 50% of human cases of HCC lose PTEN expression.¹⁹ In fact, several micro-RNAs can downregulate PTEN

expression during progression of human HCC.^{20,21} Here, we demonstrated that hypercholesterolemia promotes tumor growth by accelerating angiogenesis in *Pten* ^{Δ hep} mice. Ezetimibe lowered cholesterol levels and inhibited angiogenesis, resulting in suppression of liver tumors in *Pten* ^{Δ hep} mice on a high-fat (HF) diet.

2 | MATERIALS AND METHODS

2.1 | Animals and diets

Animal experiments were approved by the Review Boards of Jichi Medical University (17232; Tochigi, Japan) and Akita University Graduate School of Medicine (a-1-2920, b-1-2909; Akita, Japan). All animals received humane care according to the criteria outlined in the “Guide for the Care and Use of Laboratory Animals” prepared by the National Academy of Science and out institutions.

Pten^{fl/fl} mice were a generous gift from Professor Mak (University Health Network, Toronto, Canada). *Pten* ^{Δ hep} mice were generated by crossing albumin-Cre recombinase transgenic mice (Jackson Laboratory, Bar Harbor, ME, USA) and *Pten*^{fl/fl} mice.¹⁸ Albumin-Cre recombinase negative *Pten*^{fl/fl} mice (littermates) were used as control mice. Male mice were used in the present study. All mice had a C57Bl6 background and were given free access to food and water until the end of the experiments under specific pathogen-free conditions. Mice were given standard chow (CE-7; CLEA Japan, Tokyo, Japan) or an HF diet (Oriental Yeast, Tokyo, Japan) with/without ezetimibe (50 mg/kg diet) at the age of 8 weeks until 48 weeks of age. Mice were killed at the age of 48 weeks, and harvested samples were stored at -80°C until use. Externally visible tumors of diameter >2 mm were counted, with the diameter measured by stereomicroscopy. To deplete hepatic macrophages, 200 μL of liposomal clodronate (ClodronateLiposome.org, Haarlem, the Netherlands) was injected (i.p.) into mice on the HF diet, as reported previously.²² Lipid content in the HF diet is shown in Table S1. Ezetimibe was provided by Merck (Rahway, NJ, USA).

2.2 | Histology

Staining for H&E and Sirius Red were performed according to the published protocols.²⁰ Immunohistochemical (IHC) and immunofluorescent analyses were undertaken using the primary antibodies listed in Table S2 according to manufacturer instructions. The NAFLD activity score was evaluated according to the work of Kleiner et al.²³ F4/80-, NPC1L1-, Ki-67, proliferating cell nuclear antigen (PCNA)-, vascular endothelial growth factor (VEGF)- and cluster of differentiation (CD)-31-positive cells were counted on 40-50 high power ($\times 400$) fields per slide, and cell numbers and the labeling index were compared. The Sirius Red-positive area was measured on 10 magnified ($\times 100$) fields/slide and quantified using the National Institutes of Health imaging software program. As reported previously,²² the diagnosis of HCC and cholangiocellular carcinoma (CCC) was made upon positive staining for α -fetoprotein and cytokeratin-19, respectively.

2.3 | Quantitative real-time PCR

RNA was extracted from the liver and cells using TRIzol (Life Technologies Japan, Tokyo, Japan). The extracted RNA was converted to cDNA by reverse transcription. The cDNA was then subjected to PCR using the primers listed in Table S3 and LightCycler 480 SYBR Green I Master (Roche Diagnostics, Basel, Switzerland). Gene expression was normalized to that of 18S RNA as an internal control.

2.4 | Measurement of lipids, serum levels of glutamate-pyruvate transaminase, vascular endothelial growth factor, blood glucose and insulin

Hepatic lipids were isolated as described previously.²² Total cholesterol, free cholesterol, triglycerides (TG) and free fatty acids were measured using Cholesterol E (catalog number 439-17501), Free Cholesterol E (435-35801), Triglyceride E (432-40201) and

Non-Esterified Fatty Acid C (279-75401) kits, respectively, according to manufacturer (Wako Pure Chemical Industries, Osaka, Japan) instructions. Serum glutamate-pyruvate transaminase (GPT) levels were measured using a Transaminase CII Kit (431-30901) according to manufacturer (Wako Pure Chemical Industries) instructions. Blood glucose was measured using an ACCU-CHEK glucometer (Roche Diagnostics). Serum levels of insulin and VEGF were measured using enzyme-linked immunosorbent assay kits (AKRIN-031 and BMS619/2, respectively) according to manufacturer (Shibayagi, Gunma, Japan; eBioscience, San Diego, CA, USA) instructions.

2.5 | Isolation and culture of hepatic macrophages and a cell line

Hepatic macrophages were isolated from control *Pten^{fl/fl}* mice, as reported previously.²² Cells (1×10^5) were seeded onto a single well of a 12-well dish and treated with 5-50 $\mu\text{g}/\text{mL}$ low-density lipoprotein cholesterol (LDL-C; L7914; Sigma-Aldrich, Saint Louis, MO, USA) or

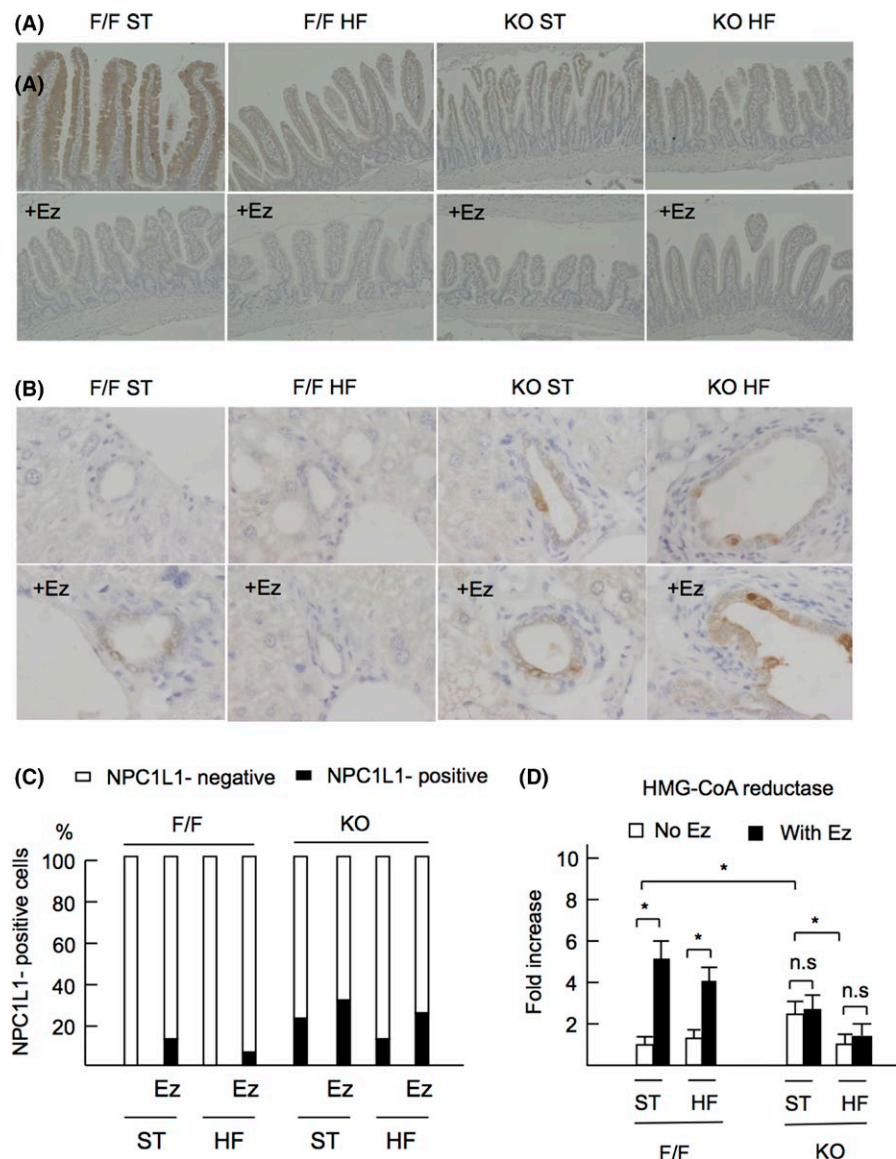


FIGURE 1 Expression of NPC1L1 and HMG-CoA reductase. *Pten^{Δhep}* mice (KO) and control *Pten^{fl/fl}* mice (F/F) were fed a standard (ST) diet or a high-fat (HF) diet with/without ezetimibe (Ez). Immunohistochemical (IHC) analyses for NPC1L1 in the ileum (A, magnification $\times 200$) and in the liver (B, magnification $\times 400$). C, Percentage of NPC1L1-positive bile-duct cells. D, Gene expression of HMG-CoA reductase examined by quantitative real-time PCR. The values were compared with gene expression of control *Pten^{fl/fl}* mice fed a standard diet. Data are the mean \pm SE. * $P < .05$, n.s., not significant

with 10–1000 µg/mL cholesterol (C3045; Sigma–Aldrich). Ezetimibe was used at 1 µmol/L in culture. Samples were harvested 8 hours or 24 hours after stimulation for mRNA and protein measurement, respectively. Huh7, a human hepatoma cell line, was used for cell proliferation assay according to manufacturer (MTT assay kit, Millipore, Temecula, CA, USA) instructions.

2.6 | Statistical analyses

Statistical analyses were carried out using one-way ANOVA or the Mann-Whitney *U*-test. Analyses were done employing SPSS v9.67 (IBM, Armonk, NY, USA). A value of *P* < .05 was considered significant.

3 | RESULTS

3.1 | NPC1L1 expression in the intestine and the liver

Studies have shown that NPC1L1 functions in the intestine and liver in humans but is limited to the intestine in mice.²⁴ Thus, we first examined intestinal and hepatic expression of NPC1L1, the target of ezetimibe, in our model using IHC analyses. As previously reported, NPC1L1 was strongly expressed in the jejunum (data not shown) and the ileum (Figure 1A) of control *Pten^{fl/fl}* mice on the standard diet, and was weakly expressed in control *Pten^{fl/fl}* mice on HF diet and in *Pten^{Δhep}* mice regardless of diet. In contrast,

TABLE 1 Metabolic parameters in mice

Diet (40W)	F/F				KO			
	ST	ST + Ez	HF	HF + Ez	ST	ST + Ez	HF	HF + Ez
Number	n = 11	n = 11	n = 10	n = 12	n = 10	n = 11	n = 10	n = 13
BW (g, end point)	32.6 ± 1.32	31.1 ± 5.20	50.8 ± 7.48 ^a	38.5 ± 7.54 ^b	29.2 ± 2.89	27.5 ± 2.20	27.7 ± 2.01	26.7 ± 2.29
Liver weight (g)	1.57 ± .10	1.36 ± .24	2.93 ± .83 ^a	1.50 ± .45 ^b	3.99 ± .76	3.28 ± .65	4.11 ± .55	3.08 ± .71 ^d
Liver/BW (%)	4.82 ± .25	4.42 ± .78	5.66 ± .95 ^a	3.85 ± .41 ^b	13.7 ± 2.85	11.9 ± 1.89	14.9 ± 2.09 ^c	11.5 ± 2.36 ^d
Epididymal fat (g)	.46 ± .10	.54 ± .26	1.61 ± .38 ^a	1.36 ± .45 ^{a,b}	.25 ± .07	.29 ± .06	.39 ± .11	.30 ± .15
Fat/BW (%)	1.34 ± .33	1.68 ± .62	3.23 ± .87 ^a	3.51 ± .77 ^a	.85 ± .25	1.06 ± .25	1.41 ± .37	1.10 ± .50
Serum								
TG (mg/dL)	50.1 ± 10.9	27.6 ± 6.38 ^a	80.7 ± 23.5 ^a	38.5 ± 15.3 ^b	26.4 ± 10.6	23.0 ± 14.7	46.8 ± 9.37	42.2 ± 11.0
TC (mg/dL)	50.6 ± 11.5	28.2 ± 5.17 ^a	231 ± 55.8 ^a	152 ± 19.0 ^{a,b}	122 ± 32.9	111 ± 25.7	259 ± 42.0 ^c	127 ± 31.5 ^d
FC (mg/dL)	16.5 ± 4.00	7.40 ± 1.61 ^a	67.5 ± 15.7 ^a	38.1 ± 3.99 ^{a,b}	29.6 ± 8.72	30.5 ± 8.78	71.4 ± 7.61 ^c	35.0 ± 5.66 ^d
FFA (mmol/L)	.14 ± .01	.13 ± .02	.40 ± .04 ^a	.27 ± .06 ^{a,b}	.18 ± .03	.14 ± .03	.28 ± .03 ^c	.26 ± .05
Liver								
TG (mg/g liver)	496 ± 101	456 ± 57.2	912 ± 281 ^a	680 ± 308 ^b	1352 ± 351	1204 ± 282	1407 ± 328	1120 ± 414
TC (mg/g liver)	53.2 ± 15.4	41.5 ± 20.5	81.2 ± 40.7	68.7 ± 34.9 ^b	102 ± 27.3	90.6 ± 14.2	116 ± 70.3	107 ± 53.4
FC (mg/g liver)	28.0 ± 11.0	19.4 ± 10.7	78.7 ± 37.9 ^a	49.5 ± 24.2 ^{a,b}	80.7 ± 32.9	64.3 ± 24.1	111 ± 69.1	79.3 ± 30.7
FFA (mmol/g liver)	1.51 ± .33	1.36 ± .17	1.57 ± .49	1.28 ± .52	2.55 ± 1.18	2.26 ± .49	2.06 ± .94	1.66 ± .50
BS (mg/dL)	133 ± 10.0	132 ± 4.94	178 ± 23.4 ^a	128 ± 13.7 ^b	115 ± 15.2	110 ± 37.3	97.8 ± 10.6	101 ± 8.07
Insulin (µU/mL)	3.00 ± .01	3.66 ± .80	12.4 ± 6.45 ^a	4.93 ± 1.55 ^b	2.54 ± .92	2.63 ± .29	2.30 ± .39	2.12 ± .53
HOMA-IR	.94 ± .07	1.20 ± .30	6.37 ± 2.91 ^a	1.59 ± .64 ^b	.72 ± .24	.71 ± .23	.55 ± .05 ^c	.52 ± .09 ^c

BS, Blood sugar; BW, body weight; FC, Free-cholesterol; FFA, Free fatty acid; HOMA-IR, insulin resistance as determined by homeostasis model assessment; TC, Total cholesterol; TG, Triglyceride.

The control *Pten^{fl/fl}* mice (F/F) and The *Pten^{Δhep}* mice (KO) were fed a standard chow (ST) or a high fat (HF) diet with/without ezetimibe (Ez).

^aSignificantly different from F/F mice on the ST.

^bSignificantly different from F/F mice on the HF diet.

^cSignificantly different from KO mice on the ST.

^dSignificantly different from KO mice on the HF diet.

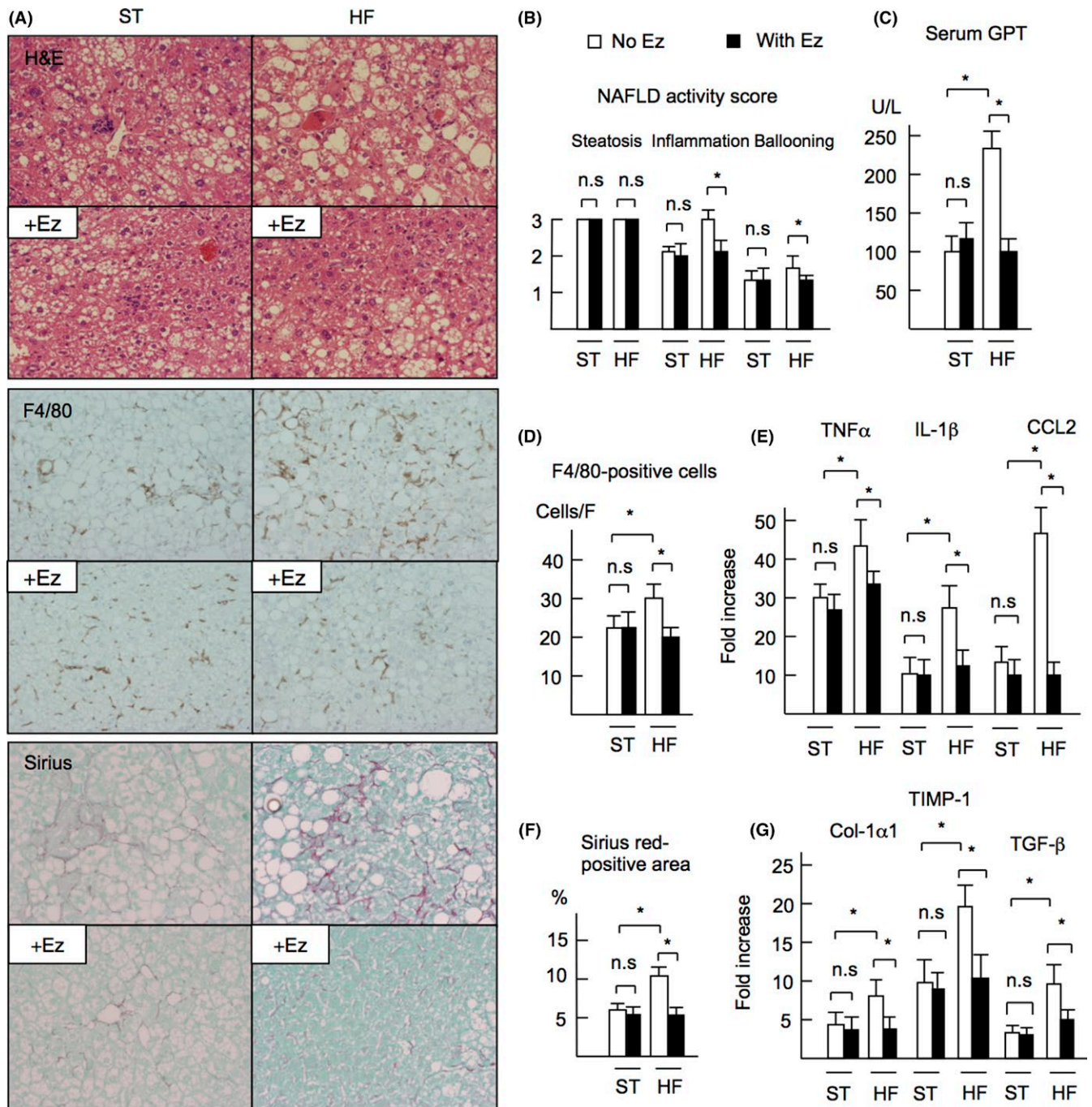


FIGURE 2 *Pten*^{Δhep} mice were fed a standard diet (ST) or a high-fat (HF) diet with/without ezetimibe (Ez) for 40 weeks. A, Liver histology. H&E staining, IHC analyses for F4/80 and Sirius Red staining are shown for assessment of general histology, inflammation and liver fibrosis, respectively (each magnification ×400). B, NAFLD activity score. C, Serum glutamate-pyruvate transaminase (GPT) levels. D, The numbers of F4/80-positive cells in a magnified field (×400). E, Gene expression of the pro-inflammatory markers TNFα, IL-1β and CCL2 examined by quantitative real-time PCR. The values were compared with gene expression of control *Pten*^{fl/fl} mice fed a standard diet. F, The Sirius Red-positive area. G, Gene expression of pro-fibrogenic markers, including collagen 1α1, TIMP-1 and TGF-β, examined by quantitative real-time PCR. The values were compared with gene expression of control *Pten*^{fl/fl} mice fed a standard diet. Data are the mean ± SE. **P* < .05, n.s., not significant

ezetimibe treatment decreased NPC1L1 expression in both control *Pten*^{fl/fl} mice and *Pten*^{Δhep} mice regardless of diet (Figure 1B). We then examined the NPC1L1 expression in the liver. NPC1L1 expression was not observed in control *Pten*^{fl/fl} mice (Figure 1B). In contrast, bile-duct cells expressed NPC1L1 in *Pten*^{Δhep} mice

on the standard diet, and 27.0% of bile-duct cells were positive for NPC1L1 staining (Figure 1B,C). NPC1L1 expression was observed even when *Pten*^{Δhep} mice were fed an HF diet, in which approximately 30% of bile-duct cells were positive for NPC1L1 (Figure 1C). In contrast to NPC1L1 expression in the ileum,

ezetimibe treatment increased the number of NPC1L1-positive cells in the bile duct cells in both control *Pten^{fl/fl}* mice and *Pten^{Δhep}* mice (Figure 1B,C).

We also examined the hepatic expression of 3-hydroxy-3-methylglutaryl-coenzyme A (HMG-CoA) reductase, an enzyme for cholesterol synthesis. Ezetimibe treatment increased the expression of HMG-CoA reductase in control *Pten^{fl/fl}* mice (Figure 1D). In *Pten^{Δhep}* mice, the expression of HMG-CoA reductase was increased in the standard diet group but not the HF diet group. In addition, ezetimibe treatment did not induce the expression of HMG-CoA reductase in *Pten^{Δhep}* mice. These data suggested that NPC1L1 expression in the bile ducts was induced when intestinal cholesterol absorption was blocked. In addition, these data suggested that biliary cholesterol was absorbed from the bile ducts in response to cholesterol requirement in mice, as observed in humans.

3.2 | Ezetimibe reduces cholesterol levels and improves steatohepatitis in *Pten^{Δhep}* mice on the high-fat diet

Fat overload has been shown to promote NASH progression in an experimental model.³ Hence, we examined the effect of the HF diet on steatohepatitis in *Pten^{Δhep}* mice. The HF diet increased the liver/body weight (%). In addition, the HF diet increased serum levels of cholesterol, but not those of TG, in *Pten^{Δhep}* mice (Table 1). The severity of inflammation and hepatocyte ballooning was exacerbated, and the NAFLD activity score was increased by consumption of the HF diet (Figure 2A,B). In accordance with enhanced inflammation as determined by H&E staining, the HF diet increased serum GPT levels further (Figure 2C), as well as the number of F4/80-positive hepatic macrophages (Figure 2A,D) and gene expression of pro-inflammatory cytokines (Figure 2E), in *Pten^{Δhep}* mice. Moreover, HF feeding promoted liver fibrosis as examined by Sirius Red staining (Figure 2A,F) and increased gene expression of pro-fibrogenic factors, including collagen 1 α 1, tissue inhibitor of metalloproteinases-1 and transforming growth factor-beta, in *Pten^{Δhep}* mice (Figure 2G).

Next, we assessed the effect of ezetimibe on steatohepatitis severity in *Pten^{Δhep}* mice. Although ezetimibe did not alter body weight, it decreased the liver weight in *Pten^{Δhep}* mice on the HF diet (Table 1). Although hepatic and serum levels of TG and free fatty acids were not altered by ezetimibe treatment, ezetimibe decreased cholesterol levels in the serum and liver (Table 1). In addition, ezetimibe suppressed infiltration of inflammatory cells and hepatocyte ballooning (Figure 2A,B), serum GPT levels (Figure 2C), the number of F4/80-positive hepatic macrophages (Figure 2D), gene expression of pro-inflammatory cytokines (Figure 2E) and liver fibrosis (Figure 2A,F,G) in *Pten^{Δhep}* mice on the HF diet. In contrast to the HF-diet group, ezetimibe did not improve steatohepatitis in the standard-diet group (Figure 2A-G). Although food intake was decreased in the HF-diet group compared with the standard-diet group, ezetimibe did not alter food intake regardless of the diet consumed (Table S4).

3.3 | Ezetimibe suppresses tumor growth in *Pten^{Δhep}* mice on the high-fat diet

Next, we looked at the effects of the HF diet and ezetimibe on the growth of liver tumors. *Pten^{Δhep}* mice on the standard diet developed precancerous adenomas, followed by HCC and CCC, as reported previously.^{18,25} The prevalence of macroscopic liver tumors reached 100% in standard and HF-diet groups at 48 weeks of age. In accordance with advanced steatohepatitis, tumor growth (as determined by the number and diameter of tumors) was increased by the HF diet compared with that by the standard diet (Figure 3A,B). Next, we assessed the effect of ezetimibe on tumor growth in *Pten^{Δhep}* mice. In the standard-diet group, ezetimibe had little effect on the development or growth of tumors. In contrast, ezetimibe suppressed the number and diameter of liver tumors in the HF-diet group (Figure 3A,B). Insulin can promote tumor growth, so we measured levels of glucose and insulin. In contrast to albumin Cre-negative *Pten^{fl/fl}* control mice, *Pten^{Δhep}* mice exhibited lower levels of glucose, insulin and Homeostatic Model Assessment of Insulin Resistance (HOMA-IR) compared with those in control mice. Although the HF diet lowered HOMA-IR further in *Pten^{Δhep}* mice, ezetimibe did not affect glucose and insulin levels or HOMA-IR in *Pten^{Δhep}* mice (Table 1).

Next, we examined tumor-cell proliferation using IHC analyses for Ki67 and PCNA. In precancerous adenoma, the index of Ki67-positive and PCNA-positive cells was increased significantly in the HF-diet group compared with those in the standard-diet group (Figure 3C,D). Ezetimibe significantly decreased the number of Ki67-positive and PCNA-positive cells in *Pten^{Δhep}* mice on the HF diet (Figure 3C,D).

We also examined whether ezetimibe affects cell proliferation of cancer cells in vitro. Ezetimibe did not promote or inhibit proliferation of Huh7, a hepatoma cell line, with/without LDL-cholesterol (data not shown). These data suggest that other factors are involved in cell proliferation of cancer cells.

3.4 | Ezetimibe inhibits angiogenesis induced by fat overload in *Pten^{Δhep}* mice

We next examined the prevalence of HCC in HF diet and the ezetimibe groups. Although most of the liver tumors in *Pten^{Δhep}* mice on the standard diet were precancerous adenoma at 48 weeks of age, the HF diet increased the prevalence of HCC at the same age (Figure 4A). Ezetimibe decreased the development of HCC at the age of 48 weeks (Figure 4A). However, ezetimibe treatment did not predispose these tumors to CCC (Figure 4A).

Hepatocellular carcinoma is characterized by high vascularity, which is a therapeutic target for HCC. Thus, we examined angiogenesis in *Pten^{Δhep}* mice. The density of VEGF-positive cells was high at the circumference of HCC tissue (Figure 4B). In contrast, the VEGF-positive cells were scarcely found in CCC tissue (Figure 4B). The density of CD31-positive cells in HCC was higher than that in CCC (Figure 4B,C). The CD31-positive cells

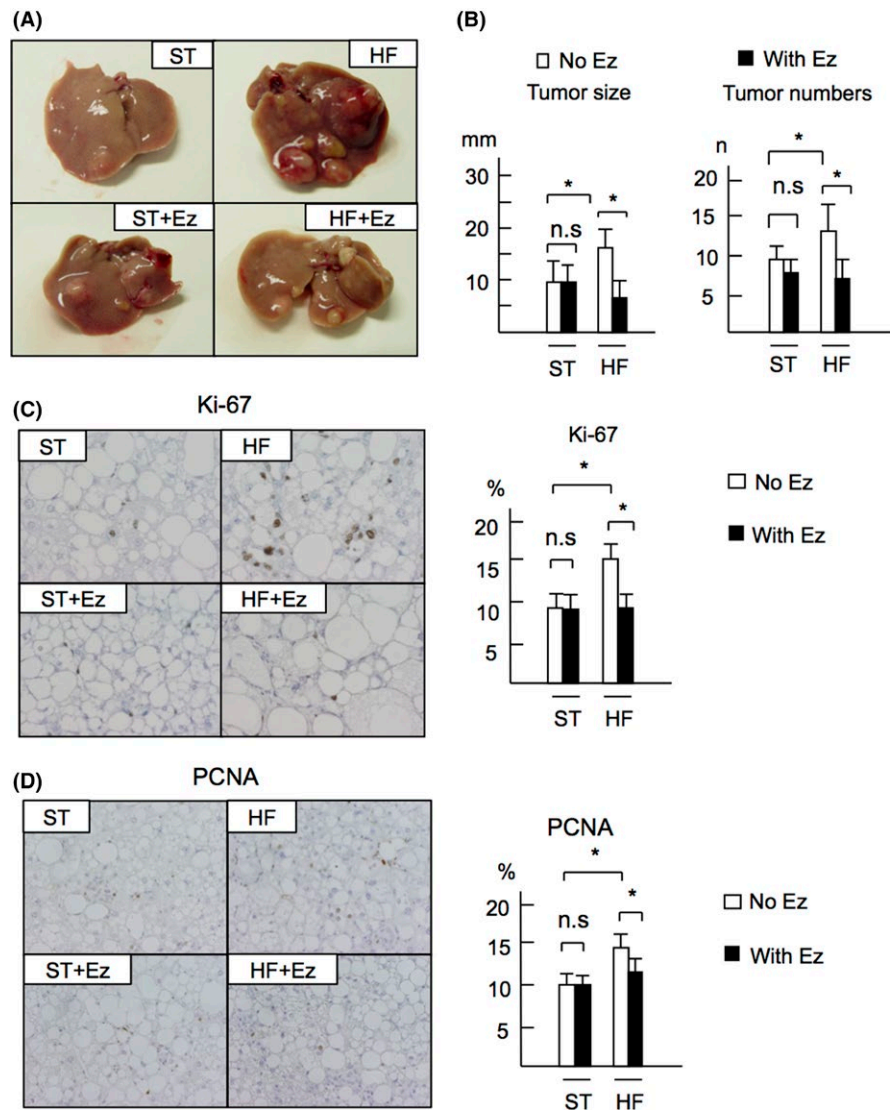


FIGURE 3 *Pten*^{Δhep} mice were fed a standard diet (ST) or a high-fat (HF) diet with/without ezetimibe (Ez) for 40 weeks. A, Representative photographs of the liver. B, Tumor diameter and numbers. C, D, Immunohistochemical (IHC) analyses for Ki67 (C) and proliferating cell nuclear antigen (PCNA) (D) (each magnification ×400)

were increased in HCC once the tumor developed in *Pten*^{Δhep} mice regardless of diet or the presence of ezetimibe. To determine the effect of HF diet, we also examined angiogenesis in precancerous tumor and non-tumor tissues. In precancerous tumor tissues, the number of VEGF-positive cells was increased by the HF diet. The numbers of VEGF-positive cells in liver sinusoids were increased by feeding on the HF diet, even in non-tumor tissues (Figure 4D,E). Serum VEGF levels were increased in *Pten*^{Δhep} mice on the HF diet compared with mice on the standard diet (Figure 4F). In accordance with increased VEGF levels, the number of endothelial cells, determined by the number of CD-31-positive cells, was increased in tumor tissue in *Pten*^{Δhep} mice on the HF diet (Figure 4D,E).

Next, we examined the effect of ezetimibe on angiogenesis in precancerous tumor tissues. Ezetimibe decreased the number of VEGF-positive and CD31-positive cells in tumors of *Pten*^{Δhep} mice on the HF diet (Figure 4D,E). In accordance with IHC analyses, ezetimibe decreased VEGF levels in *Pten*^{Δhep} mice on the HF diet significantly ($P < .05$) (Figure 4F). In contrast to the HF diet, ezetimibe

did not affect angiogenesis in *Pten*^{Δhep} mice on the standard diet (Figure 4D-F).

3.5 | Fat overload increases hepatic expression of vascular endothelial growth factor in mice that lack inflammation and fibrosis

Inflammation and fibrosis can promote angiogenesis, so we examined whether fat overload can promote angiogenesis in mice that lack inflammation and fibrosis. In these experiments, we used albumin Cre-negative *Pten*^{ff} mice, which show a similar phenotype to wild-type mice. The HF diet induced increases in body weight (Table 1) and steatosis (Figure 5A). However, serum GPT levels were not increased in the HF-diet group (Figure 5B). In addition, gene expression of pro-inflammatory markers was not altered by the HF diet (Figure 5C). Moreover, fibrosis was not induced by the HF diet (data not shown).

A few VEGF-positive cells were observed in the standard-diet group (Figure 5D,E). The HF diet increased the number of

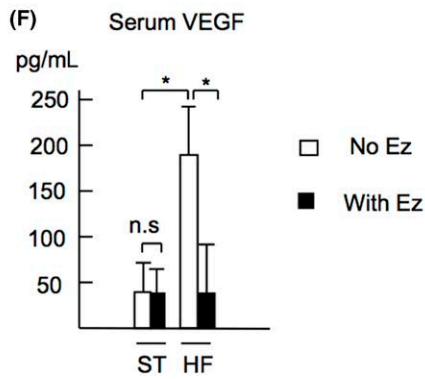
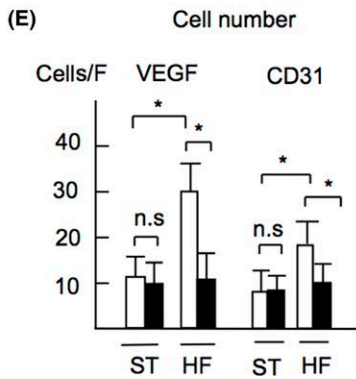
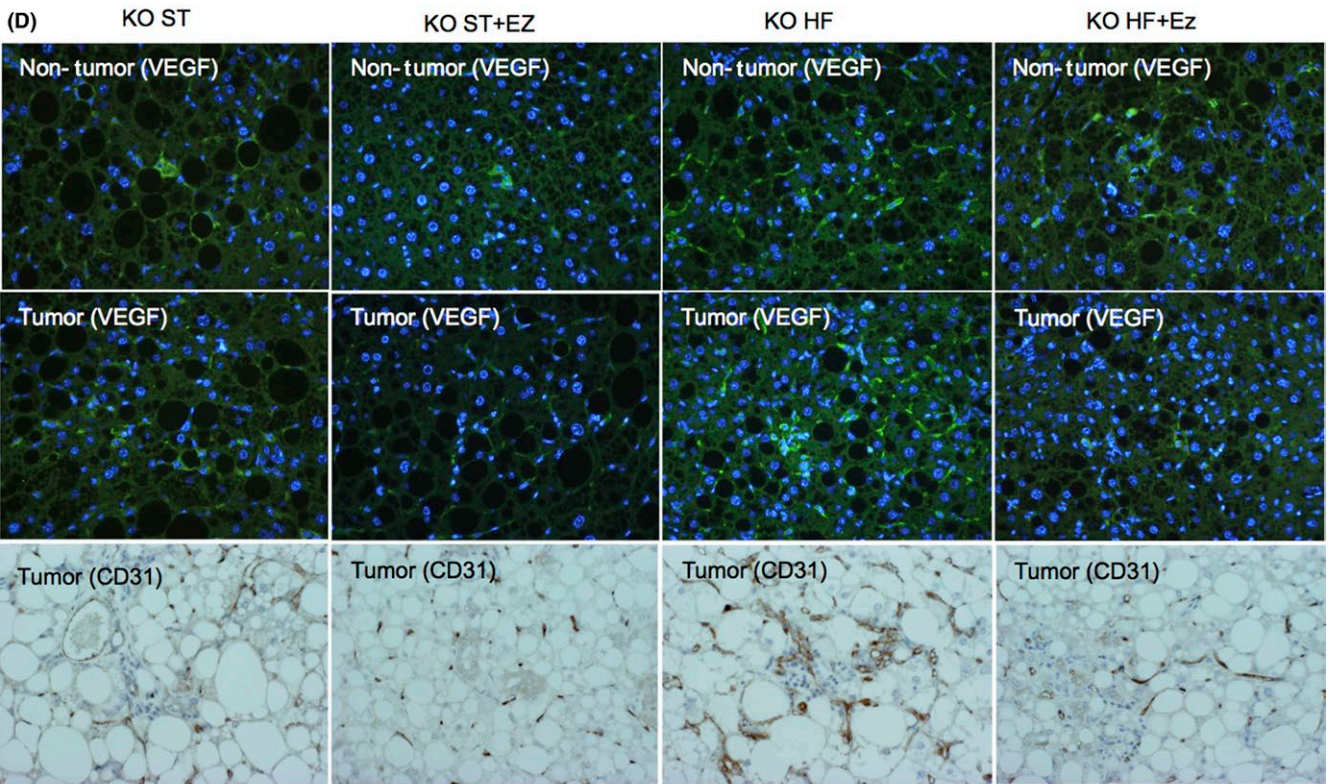
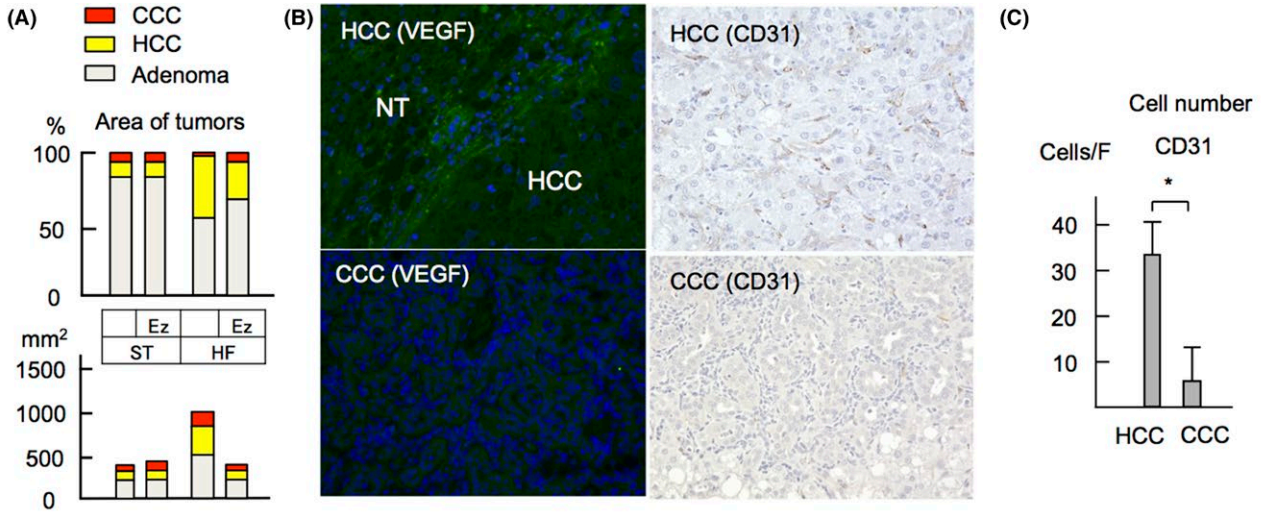


FIGURE 4 *Pten*^{Δhep} mice were fed a standard diet (ST) or a high-fat (HF) diet with/without ezetimibe (Ez) for 40 weeks. A, Area of tumors was measured using Image J. The proportion of adenoma, hepatocellular carcinoma (HCC) and cholangiocellular carcinoma (CCC) lesions are shown. B, Immunofluorescent staining for vascular endothelial growth factor (VEGF) and immunohistochemical (IHC) analyses for CD31 (each magnification ×400) in HCC and CCC. NT, non-tumor area. C, The numbers of CD31-positive cells in a magnified field (×400). D, Immunofluorescent staining for VEGF and IHC analyses for CD31 in non-tumor area and precancerous adenoma (tumor) (each magnification ×400). E, Number of VEGF-positive and CD31-positive cells. F, Serum VEGF levels. Data are the mean ± SE. **P* < .05, n.s., not significant

VEGF-positive cells in the liver (Figure 5D,E) as well as serum VEGF levels (Figure 5F), which were similar levels to those observed in *Pten*^{Δhep} mice on the HF diet. Ezetimibe reduced the body weight (Table 1) and hepatic steatosis (Figure 5A). Ezetimibe decreased the number of VEGF-positive cells and serum VEGF levels in the HF-diet group, but not in the standard-diet group (Figure 5D,E). These data suggested that fat overload promoted angiogenesis independent of inflammation. In addition, ezetimibe can inhibit the angiogenesis induced by fat overload.

3.6 | Kupffer cells increase vascular endothelial growth factor expression in response to lipoprotein-cholesterol

Next, we sought to determine the source of VEGF in the liver. Double immunofluorescent staining showed that VEGF-positive cells were mainly co-localized with F4/80, a marker for macrophages. In *Pten*^{Δhep} mice, Ly6C-positive macrophages are recruited to the liver from the bone marrow.²² However, <10% of Ly6C cells

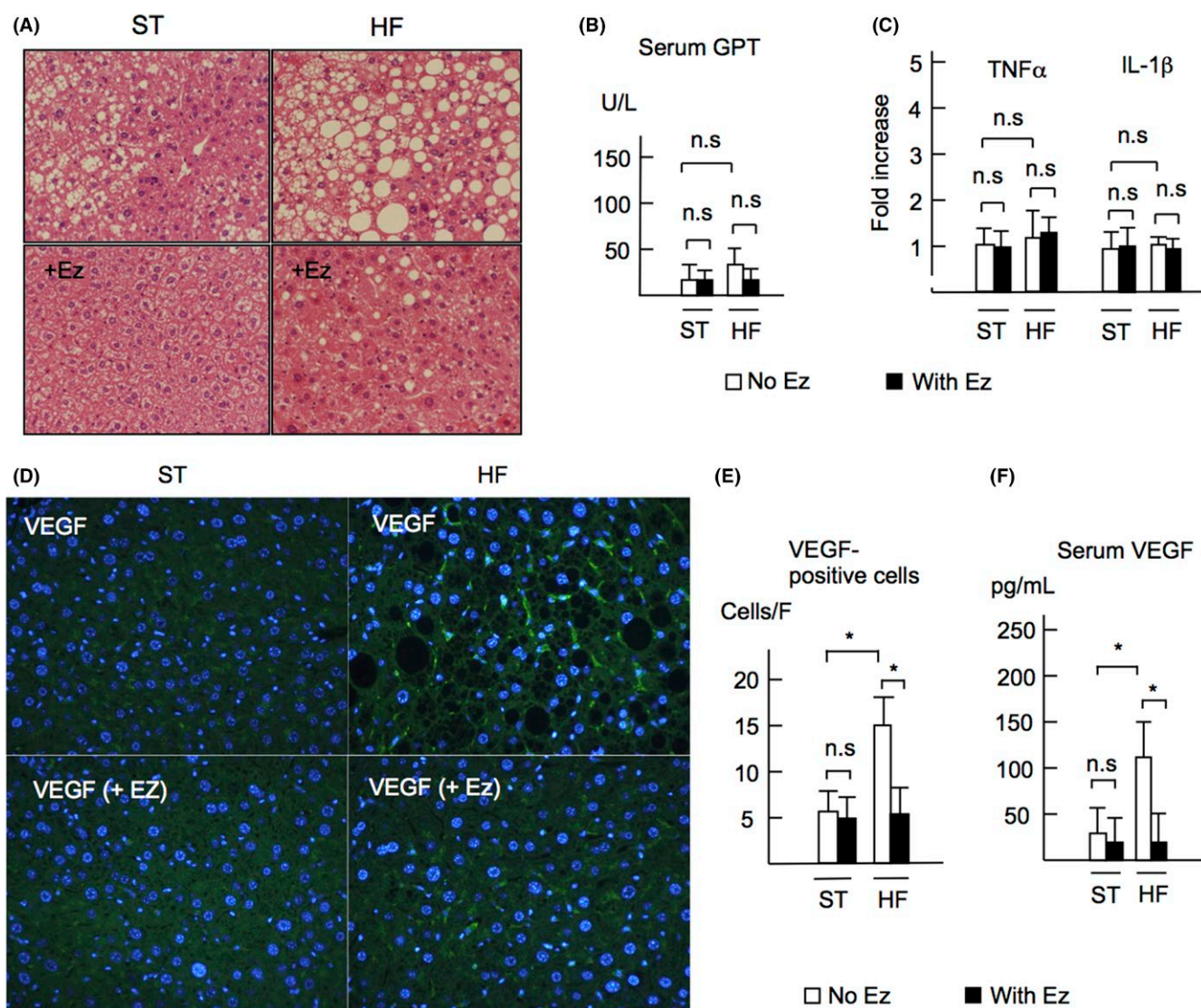


FIGURE 5 Control *Pten*^{fl/fl} mice were fed a standard diet (ST) or a high-fat (HF) diet with/without ezetimibe (Ez) for 40 weeks. A, H&E staining (magnification ×400). B, Serum GPT levels. C, Gene expression of the pro-inflammatory cytokines TNFα and IL-1β. D, Immunofluorescent staining for vascular endothelial growth factor (VEGF) (magnification ×400). E, The number of VEGF-positive cells. F, Serum VEGF levels. Data are the mean ± SE. **P* < .05, n.s., not significant

were co-localized with VEGF, even though the mice were fed the HF diet (Figure 6A). Double-positive cells for α -smooth muscle actin and VEGF were <10%, suggesting that hepatic stellate cells were not the major source of VEGF. CD31-positive cells did not express VEGF, suggesting that vascular endothelial cells were not the source of VEGF. These data strongly suggested that the resident macrophages, Kupffer cells, contributed to increased VEGF levels in *Pten* ^{Δ hep} mice on the HF diet. We counted the number of cells co-localized with F4/80 and VEGF, in which 35%, 32%, 76% and 36% of cells were co-localized in the standard chow, standard chow plus ezetimibe, high fat and high fat plus ezetimibe groups, respectively. Co-localization of VEGF and F4/80 was also observed in control mice on the HF diet (Figure 6B). To confirm VEGF production from Kupffer cells, macrophages were depleted using a single injection of liposomal clodronate. Macrophage depletion decreased VEGF levels in mice on the HF diet (Figure 6C), suggesting that Kupffer cells were the major source of VEGF in response to the HF diet.

Next, we examined the effects of cholesterol and ezetimibe on VEGF expression in Kupffer cells isolated from albumin Cre-negative *Pten*^{fl/fl} mice. LDL-cholesterol overload increased VEGF at mRNA and protein levels in Kupffer cells (Figure 6D,E) but cholesterol without a lipoprotein did not (data not shown). We also tested whether ezetimibe can decrease VEGF levels in vitro. However, ezetimibe did not

decrease VEGF levels induced by LDL-cholesterol (Figure 6D,E). An immunofluorescent study showed that Kupffer cells did not express NPC1L1 under the presence of LDL-cholesterol, cholesterol without lipoprotein or ezetimibe (data not shown). These data suggested that ezetimibe did not act directly on Kupffer cells.

4 | DISCUSSION

In the present study, we demonstrated that an HF diet promoted the progression of steatohepatitis as well as tumor growth in *Pten* ^{Δ hep} mice, in which hypercholesterolemia is associated with augmented angiogenesis. In these *Pten* ^{Δ hep} mice with hypercholesterolemia, ezetimibe treatment suppressed the severity of steatohepatitis and tumor growth by inhibiting angiogenesis. During angiogenesis, hepatic macrophage Kupffer cells produced VEGF in response to cholesterol overload in mice.

As reported by Shearn et al,²⁶ an HF diet can enhance hepatic inflammation in *Pten* ^{Δ hep} mice. Here, we demonstrated further that fat overload promoted liver fibrosis as well as tumor growth in *Pten* ^{Δ hep} mice, which were not examined in the study by Shearn et al.²⁶ This is because the duration of the HF diet was longer in our study (40 weeks vs 6 weeks). Cholesterol is a key lipid that promotes

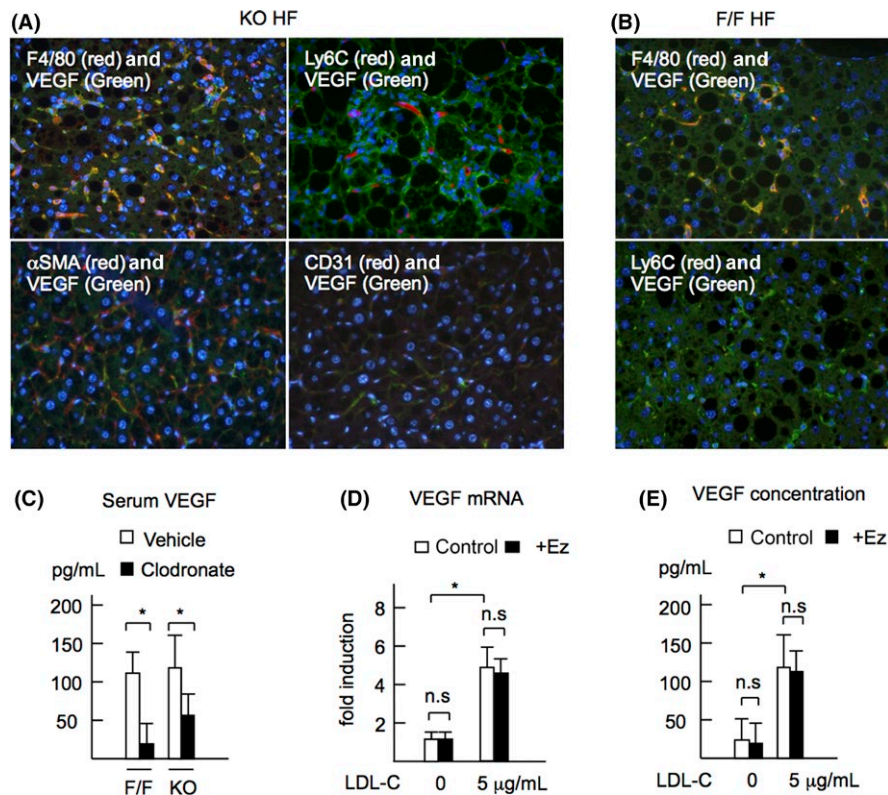


FIGURE 6 A, *Pten* ^{Δ hep} mice (KO) were fed a high-fat (HF) diet for 40 weeks. Immunofluorescent staining for F4/80, Ly6C, α -smooth muscle actin (α SMA), CD31 and vascular endothelial growth factor (VEGF) (each magnification \times 400). B, Control *Pten*^{fl/fl} mice (F/F) were fed a HF diet for 40 weeks. Immunofluorescent staining for F4/80, Ly6C and VEGF (each magnification \times 400). C, *Pten* ^{Δ hep} mice and control *Pten*^{fl/fl} mice on the high-fat (HF) diet were injected with liposomal clodronate to deplete hepatic macrophages. Serum VEGF levels are shown. D, E, Hepatic macrophages were stimulated with LDL-cholesterol (LDL-C) at 5 μ g/mL. (D) Gene expression of VEGF. F, VEGF concentration in the supernatant. Data are the mean \pm SE. * P < .05, n.s., not significant

the progression of steatohepatitis and tumors. In *Pten^{Δhep}* mice, levels of cholesterol increased in the serum and liver during consumption of the HF diet rather than TG. Ezetimibe reduced cholesterol levels significantly compared with those of TG, suggesting that excess cholesterol contributes to the progression of steatohepatitis as well as tumors. In patients with cryptogenic cirrhosis who develop HCC later, serum cholesterol levels are higher than those of control groups.²⁷ In contrast, a low cholesterol level is associated with a high incidence of HCC in patients with chronic infection with the hepatitis B virus.²⁸ In patients with chronic hepatitis B virus infection, low cholesterol levels reflect an advanced stage of liver disease, in which cholesterol synthesis is impaired in hepatocytes. These data suggest that the role of cholesterol in HCC development differs among the types of liver disease.

We showed, for the first time, that ezetimibe decreased tumor growth in the liver. We considered the primary effect of ezetimibe to be lowering of serum cholesterol levels. In an experimental NASH model using STAM mice, ezetimibe failed to reduce tumor development in the liver.²⁹ However, STAM mice developed hyperglycemia but not hypercholesterolemia, suggesting that the toxic effect of glucose was the primary cause of injury in STAM mice. Levels of glucose and insulin were not increased in *Pten^{Δhep}* mice regardless of diet and ezetimibe treatment. Therefore, the beneficial effects of ezetimibe are expected if lipid toxicity is the primary cause of steatohepatitis. In a clinical trial, ezetimibe also failed to reduce fatty livers in the Magnetic Resonance Imaging and Elastography in Ezetimibe Versus Placebo for the Assessment of Response to Treatment in NASH (MOZART) Trial.¹⁷ The cholesterol levels in patients with NASH enrolled in the MOZART Trial were lower than those in a Japanese study¹⁶ in which ezetimibe showed beneficial effects in patients with NASH and hypercholesterolemia. Thus, ezetimibe may show an optimal performance in patients with hypercholesterolemia.

Initially, we speculated that ezetimibe could reduce the number of liver tumors in *Pten^{Δhep}* mice on the standard diet because *Pten^{Δhep}* mice showed increased cholesterol levels compared with control *Pten^{fl/fl}* mice.¹⁸ However, ezetimibe did not ameliorate the severity of steatohepatitis or tumor growth in the standard-diet group. Similar effects of ezetimibe have been noted in other tumor-bearing models if mice are fed a low-fat, low-cholesterol diet.³⁰ Although PTEN deficiency can increase cholesterol synthesis by activating the mammalian target of rapamycin and its downstream targets PPAR- γ , *srebp-1* and *srebp-2*,³¹ the increase in serum cholesterol levels was mild in *Pten^{Δhep}* mice. Thus, ezetimibe might have minimal effects on tumor suppression if cholesterol levels are not sufficiently high. However, statins have the potential to suppress tumors in *Pten^{Δhep}* mice on the standard diet because PTEN deficiency in hepatocytes showed increased expression of HMG-CoA reductase, a target of statin.

One of the mechanisms by which ezetimibe suppresses HCC is inhibition of cholesterol-mediated angiogenesis. We showed that hypercholesterolemia induced VEGF production in the liver. Even in control mice, the HF diet increased serum levels of cholesterol

and VEGF, suggesting that hypercholesterolemia contributes to VEGF production. In contrast, ezetimibe did not affect angiogenesis in *Pten^{Δhep}* mice on the standard diet, in which the increase in cholesterol level was mild. Hypercholesterolemia also promotes angiogenesis and subsequent tumor growth in other types of malignancy, including breast tumors³⁰ and prostatic cancers.³² NASH is characterized by increased angiogenesis³³ and inhibition of angiogenesis suppresses NASH severity.¹² Thus, hypercholesterolemia might be a risk factor for HCC in NASH. Hypercholesterolemia also enhanced hepatic inflammation, a potent promoter of angiogenesis,³⁴ in *Pten^{Δhep}* mice on the HF diet. During angiogenesis, hepatic macrophages produce VEGF owing to cholesterol overload. Of the several types of cells that produce VEGF in the liver, Kupffer cells have been reported to express VEGF in response to liver injuries.³⁵ Although we examined NPC1L1 expression in Kupffer cells, NPC1L1 was not detected. Indeed, ezetimibe did not change cholesterol-induced VEGF production in Kupffer cells. Seedorf et al³⁶ showed that ezetimibe blocked cholesterol uptake in macrophages, suggesting that different types of macrophages can express NPC1L1 or other receptors that can engage with ezetimibe.

We demonstrated that ezetimibe could reduce VEGF production by lowering cholesterol levels, as observed in statins.¹³ Ezetimibe also improved hyperglycemia and hyperinsulinemia as a secondary effect in HF diet-fed control mice, in which glucose and insulin are potent inducers of VEGF.^{37,38} Recently, ezetimibe has been reported to possess additional functions, including alteration of gut microbiota³⁹ and autophagy,⁴⁰ which are closely associated with steatohepatitis and liver tumors. Thus, these beneficial effects of ezetimibe may also contribute to the suppression of liver tumors arising from steatohepatitis.

In conclusion, our data demonstrated that ezetimibe reduced HCC by inhibiting angiogenesis in *Pten^{Δhep}* mice with hypercholesterolemia. These findings may have clinical implications because ezetimibe is used as a cholesterol-lowering agent. Clinical trials are necessary to assess the ability of ezetimibe to reduce human HCC related to steatohepatitis.

ACKNOWLEDGMENTS

We thank Professor Tak W Mak (University Health Network, Toronto, Canada) for his generous gift of *Pten^{fl/fl}* mice. We also thank Masako Watanabe, Yuko Terada and Miho Sashikawa (All Jichi Medical University) and for their excellent technical assistance. We thank Arshad Makhdum from Edanz Group (www.edanzediting.com/ac) for editing a draft of this manuscript.

CONFLICT OF INTEREST

Hirohide Ohnishi received research fees from Bayer Yakuhin, who had no role in the design, execution, analyses or interpretation of the present study. The rest of authors have no conflict of interests in the present study.

ORCID

Kouichi Miura  <https://orcid.org/0000-0001-8036-6544>

REFERENCES

- Wong RJ, Aguilar M, Cheung R, et al. Nonalcoholic steatohepatitis is the second leading etiology of liver disease among adults awaiting liver transplantation in the United States. *Gastroenterology*. 2015;148:547-555.
- Ferolla SM, Silva LC, Ferrari Mde LA, et al. Dietary approach in the treatment of nonalcoholic fatty liver disease. *World J Hepatol*. 2015;7:2522-2534.
- Matsuzawa N, Takamura T, Kurita S, et al. Lipid-induced oxidative stress causes steatohepatitis in mice fed an atherogenic diet. *Hepatology*. 2007;46:1392-1403.
- Puri P, Baillie RA, Wiest MM, et al. A lipidomic analysis of nonalcoholic fatty liver disease. *Hepatology*. 2007;46:1081-1090.
- Caballero F, Fernández A, De Lacy AM, Fernández-Checa JC, Caballería J, García-Ruiz C. Enhanced free cholesterol, SREBP-2 and S1A expression in human NASH. *J Hepatol*. 2009;50:789-796.
- Lai MS, Hsieh MS, Chiu YH, Chen THH. Type 2 diabetes and hepatocellular carcinoma: a cohort study in high prevalence area of hepatitis virus infection. *Hepatology*. 2006;43:1295-1302.
- Ioannou GN, Morrow OB, Connole ML, Lee SP. Association between dietary nutrient composition and the incidence of cirrhosis or liver cancer in the United States population. *Hepatology*. 2009;50:175-184.
- Marí M, Caballero F, Colell A, et al. Mitochondrial free cholesterol loading sensitizes to TNF- and Fas-mediated steatohepatitis. *Cell Metab*. 2006;4:185-198.
- Teratani T, Tomita K, Suzuki T, et al. A high-cholesterol diet exacerbates liver fibrosis in mice via accumulation of free cholesterol in hepatic stellate cells. *Gastroenterology*. 2012;142:152-164.e10
- Li Y, Schwabe RF, DeVries-Seimon T, et al. Free cholesterol-loaded macrophages are an abundant source of tumor necrosis factor- α and interleukin-6: model of NF- κ B- and map kinase-dependent inflammation in advanced atherosclerosis. *J Biol Chem*. 2005;280:21763-21772.
- Eaton CB, Gramling R, Parker DR, Roberts MB, Lu B, Ridker PM. Prospective association of vascular endothelial growth factor-A (VEGF-A) with coronary heart disease mortality in Southeastern New England. *Atherosclerosis*. 2008;200:221-227.
- Coulon S, Legry V, Heindryckx F, et al. Role of vascular endothelial growth factor in the pathophysiology of nonalcoholic steatohepatitis in two rodent models. *Hepatology*. 2013;57:1793-1805.
- Dongiovanni P, Petta S, Mannisto V, et al. Statin use and non-alcoholic steatohepatitis in at risk individuals. *J Hepatol*. 2015;63:705-712.
- El-Serag HB, Johnson ML, Hachem C, Morgana RO. Statins are associated with a reduced risk of hepatocellular carcinoma in a large cohort of patients with diabetes. *Gastroenterology*. 2009;136:1601-1608.
- Nishio T, Taura K, Nakamura N, et al. Impact of statin use on the prognosis of patients with hepatocellular carcinoma undergoing liver resection: a subgroup analysis of patients without chronic hepatitis viral infection. *Surgery*. 2017;163:264-269.
- Yoneda M, Fujita K, Nozaki Y, et al. Efficacy of ezetimibe for the treatment of non-alcoholic steatohepatitis: an open-label, pilot study. *Hepatol Res*. 2010;40:566-573.
- Loomba R, Sirlin CB, Ang B, et al. Ezetimibe for the treatment of nonalcoholic steatohepatitis: assessment by novel magnetic resonance imaging and magnetic resonance elastography in a randomized trial (MOZART trial). *Hepatology*. 2015;61:1239-1250.
- Horie Y, Suzuki A, Kataoka E, et al. Hepatocyte-specific Pten deficiency results in steatohepatitis and hepatocellular carcinomas. *J Clin Invest*. 2004;113:1774-1783.
- Hu TH, Huang CC, Lin PR, et al. Expression and prognostic role of tumor suppressor gene PTEN/MMAC1/TEP1 in hepatocellular carcinoma. *Cancer*. 2003;97:1929-1940.
- Fu X, Wen H, Jing L, et al. MicroRNA-155-5p promotes hepatocellular carcinoma progression by suppressing PTEN through the PI3K/Akt pathway. *Cancer Sci*. 2017;108:620-631.
- Shi DM, Bian XY, Qin CD, Wu WZ. miR-106b-5p promotes stem cell-like properties of hepatocellular carcinoma cells by targeting PTEN via PI3K/Akt pathway. *Onco Targets Ther*. 2018;11:571-585.
- Miura K, Ishioka M, Minami S, et al. Toll-like receptor 4 on macrophage promotes the development of steatohepatitis-related hepatocellular carcinoma in mice. *J Biol Chem*. 2016;291:11504-11517.
- Kleiner DE, Brunt EM, Van Natta M, et al. Design and validation of a histological scoring system for nonalcoholic fatty liver disease. *Hepatology*. 2005;41:1313-1321.
- Altmann SW, Davis HR, Zhu LJ, et al. Niemann-Pick C1 Like 1 protein is critical for intestinal cholesterol absorption. *Science*. 2004;303(5661):1201-1204.
- Galicia VA, He L, Dang H, et al. Expansion of hepatic tumor progenitor cells in Pten-null mice requires liver injury and is reversed by loss of AKT2. *Gastroenterology*. 2010;139:2170-2182.
- Shearn CT, Mercer KE, Orlicky DJ, et al. Short term feeding of a high fat diet exerts an additive effect on hepatocellular damage and steatosis in liver-specific PTEN knockout mice. *PLoS One*. 2014;9:e96553.
- Bugianesi E, Leone N, Vanni E, et al. Expanding the natural history of nonalcoholic steatohepatitis: from cryptogenic cirrhosis to hepatocellular carcinoma. *Gastroenterology*. 2002;123:134-140.
- Kumada T, Toyoda H, Kiriya S, et al. Incidence of hepatocellular carcinoma in patients with chronic hepatitis B virus infection who have normal alanine aminotransferase values. *J Med Virol*. 2010;82:539-545.
- Orime K, Shirakawa J, Togashi Y, et al. Lipid-lowering agents inhibit hepatic steatosis in a non-alcoholic steatohepatitis-derived hepatocellular carcinoma mouse model. *Eur J Pharmacol*. 2016;772:22-32.
- Pelton K, Coticchia CM, Curatolo AS, et al. Hypercholesterolemia induces angiogenesis and accelerates growth of breast tumors in vivo. *Am J Pathol*. 2014;184:2099-2110.
- Yue S, Li J, Lee SY, et al. Cholesteryl ester accumulation induced by PTEN loss and PI3K/AKT activation underlies human prostate cancer aggressiveness. *Cell Metab*. 2014;19:393-406.
- Solomon KR, Pelton K, Boucher K, et al. Ezetimibe is an inhibitor of tumor angiogenesis. *Am J Pathol*. 2009;174:1017-1026.
- Kitade M, Yoshiji H, Kojima H, et al. Leptin-mediated neovascularization is a prerequisite for progression of nonalcoholic steatohepatitis in rats. *Hepatology*. 2006;44:983-991.
- Ehling J, Bartneck M, Wei X, et al. CCL2-dependent infiltrating macrophages promote angiogenesis in progressive liver fibrosis. *Gut*. 2014;63:1960-1971.
- Ishikawa K, Mochida S, Mashiba S, et al. Expressions of vascular endothelial growth factor in nonparenchymal as well as parenchymal cells in rat liver after necrosis. *Biochem Biophys Res Commun*. 1999;254:587-593.
- Seedorf U, Engel T, Lueken A, Bode G, Lorkowski S, Assmann G. Cholesterol absorption inhibitor Ezetimibe blocks uptake of oxidized LDL in human macrophages. *Biochem Biophys Res Commun*. 2004;320:1337-1341.
- Desouza CV, Gerety M, Hamel FG. Neointimal hyperplasia and vascular endothelial growth factor expression are increased in

- normoglycemic, insulin resistant, obese fatty rats. *Atherosclerosis*. 2006;184:283-289.
38. Yoshiji H, Noguchi R, Kitade M, et al. Branched-chain amino acids suppress insulin-resistance-based hepatocarcinogenesis in obese diabetic rats. *J Gastroenterol*. 2009;44:483-491.
39. Catry E, Pachikian BD, Salazar N, Neyrinck AM, Cani PD, Delzenne NM. Ezetimibe and simvastatin modulate gut microbiota and expression of genes related to cholesterol metabolism. *Life Sci*. 2015;132:77-84.
40. Yamamura T, Ohsaki Y, Suzuki M, et al. Inhibition of Niemann-Pick-type C1-like1 by ezetimibe activates autophagy in human hepatocytes and reduces mutant α 1-antitrypsin Z deposition. *Hepatology*. 2014;59:1591-1599.

SUPPORTING INFORMATION

Additional supporting information may be found online in the Supporting Information section at the end of the article.

How to cite this article: Miura K, Ohnishi H, Morimoto N, et al. Ezetimibe suppresses development of liver tumors by inhibiting angiogenesis in mice fed a high-fat diet. *Cancer Sci*. 2019;110:771-783. <https://doi.org/10.1111/cas.13902>